OXFORD

Editor's Choice

The tumor-associated Tn antigen fosters lung metastasis and recruitment of regulatory T cells in triple negative breast cancer

María Florencia Festari, Valeria da Costa, Santiago A Rodríguez-Zraquia, Monique Costa, Mercedes Landeira, Pablo Lores, Patricia Solari-Saquieres, M Gabriela Kramer, Teresa Freire* [iD]

Laboratorio de Inmunomodulación y Desarrollo de Vacunas, Departamento de Inmunobiología, Facultad de Medicina, Universidad de La República, Montevideo, Uruguay

*Corresponding author: Tel: (598) 2924 9562; Fax: (598) 2924 9563; e-mail: tfreire@fmed.edu.uy

Cancer is a leading cause of death worldwide, accounting for nearly 10 million deaths. Among breast cancers (BC) subtypes, triple-negative (TN) BC is characterized by metastatic progression and poor patient prognosis. Although TNBC is initially sensitive to chemotherapy, many TNBC patients rapidly develop resistance, at which point metastatic disease is highly lethal. Cancer cells present phenotypic changes or molecular signatures that distinguish them from healthy cells. The Tn antigen (GalNAc-O-Thr/Ser), which constitutes a powerful tool as tumor marker, was recently reported to contribute to tumor growth. However, its role in BC-derived metastasis has not yet been addressed. In this work, we generated a pre-clinical orthotopic Tn$^+$ model of metastatic TNBC, which mimics the patient surgical treatment and is useful to study the role of Tn in metastasis and immunoregulation. We obtained two different cell clones, which differed in their Tn antigen expression: a high Tn-expressing and a non-expressing clone. Interestingly, the Tn-positive cell line generated significantly larger tumors and higher degree of lung metastases associated with a lower survival rate than the Tn-negative and parental cell line. Furthermore, we also found that both tumors and draining-lymph nodes from Tn$^+$-tumor-bearing mice presented a higher frequency of CD4$^+$ FoxP3$^+$ T cells, while their splenocytes expressed higher levels of IL-10. In conclusion, this work suggests that the Tn antigen participates in breast tumor growth and spreading, favoring metastases to the lungs that are associated with an immunoregulatory state, suggesting that Tn-based immunotherapy could be a strategy of choice to treat these tumors.

Key words: immunoregulation; metastasis; Tn antigen; triple negative breast cancer; tumor growth.

Introduction

Breast cancer (BC) is the first cancer in terms of incidence among women and the main cause of death by cancer in women worldwide [https://www.who.int/cancer/ (2021)]. In the last 20 years, breast cancer mortality has continuously decreased as a result of mass screening programs and early diagnosis, but also as a consequence of improved treatment for both localized and metastatic disease (Scimeca et al. 2019; Thomas et al. 2019). Nevertheless, despite surgery and endocrine or targeted therapies, the morbidity and mortality of BC remain highest in female patients, with metastasis being invariably responsible for patient death in this type of cancer (Redig and McAllister 2013). Therefore, more research directed into this area may lead to novel biomarkers or treatments for metastasis, thereby enhancing the survival rates in breast cancer patients.

The triple negative BC (TNBC) subtype is characterized by metastatic progression, poor patient prognosis, and is identified by the absence of biomolecules that form the basis for targeted therapies for the other BC subtypes, namely estrogen receptor, progesterone receptor, and Her2 (Yin et al. 2020). It accounts for 15–20% of breast cancer cases, for which there are currently no approved targeted therapies (Yin et al. 2020). They are heterogeneous tumors

with aggressive phenotype and higher relapse rate (Abramson and Mayer 2014). Moreover, compared to other BC subtypes, TNBCs are less differentiated and prone to metastasize within 5 years of diagnosis leading to shorter overall survival of patients when compared to other BC subtypes (Giuli et al. 2019; Park et al. 2019). Finally, although TNBC is initially highly sensitive to chemotherapy, many TNBC patients rapidly develop resistance leading to highly lethal metastasis (Garrido-Castro et al. 2019).

Cancer cells present phenotypic changes or molecular signatures that distinguish them from healthy cells. Some of these signatures are glycans, being the result of a series of alterations in the glycosylation pathways of proteins or lipids on these cells (Pinho and Reis 2015; Munkley and Elliott 2016; Mereiter et al. 2019; Peixoto et al. 2019). Apart from representing tumor markers, these glycan motifs have functional implications in potentiating tumor progression, spreading and invasiveness (Freire and Osinaga 2012). In particular, the Tn antigen (GalNAc-O-Thr/Ser) has been described in most adenocarcinomas whereas it is not found in normal tissues (Chia et al. 2016; Fu et al. 2016). Thus, it constitutes a powerful tool as tumor marker, for cancer clinical diagnosis and follow-up studies (Freire et al. 2006; Freire and Osinaga 2012). Indeed, Tn levels have

prognostic value in breast, ovarian, pancreas, gastric and biliary tract cancer patients (Kolbl et al. 2016). Also, the expression of Tn has been correlated with an unfavorable clinical outcome, decreased survival of cancer patients and high metastatic potential of cancer cells (Freire and Osinaga 2012; Hofmann et al. 2015; Kolbl et al. 2016). Moreover, in vitro data have suggested that the Tn antigen might contribute to the adhesion or invasiveness of cancer cells, and consequently, participate in the metastasis process (Gill et al. 2013; Matsumoto et al. 2013; Bapu et al. 2016; Dong et al. 2018). Recent works indicate that the Tn antigen promotes human colorectal cancer metastasis and induces epithelial to mesenchymal transition of cancer cells (Liu et al. 2019). Nevertheless, the mechanisms underlying these phenomena are not completely understood, in particular whether the Tn antigen may play a causative role in the metastatic process through immune evasion in TNBC.

Tumor-associated carbohydrate antigens can shape the malignant phenotype of tumor cells or suppress anti-tumor immunity, contributing to tumor growth (Freire and Osinaga 2012; Kolbl et al. 2016). Recent studies have suggested a main role of Tn antigen in tumor growth, although xenografted experimental tumor models were used, with limitations on the study of the immune system and generation of metastases (Liu et al. 2019). However, recent data of our and other research groups, have confirmed the role of the Tn antigen favoring tumor cancer growth and immunoregulation (Dusoswa et al. 2020; da Costa et al. 2021). Nevertheless, the function of this antigen in the modulation of the immune system during the metastatic process has not been described yet. In this work, we provide evidence of the role of the Tn antigen in the TNBC-induced metastasis and in immune evasion through the generation of regulatory T cell lymphocytes.

Results
Cosmc deficiency induces the expression of Tn antigen on 4T1 cells
We first developed a Tn-expressing TNBC cell line as the main approach to understand the role of this antigen in tumor growth, metastasis and immunoregulation. Thus, Tn^+ cells were generated using the TNBC 4T1 cell line (4T1-wt) and knocking out *Cosmc* in these cells using the CRISPR/Cas9 gene editing (Figure 1A). Transfected cells were selected by eGFP expression followed by single cell deposition sorting. Two different cell clones were selected, a Tn^+ (4T1-Tn$^+$) and a Tn^- (4T1-Tn$^-$). The expression of Tn was analyzed by recognition with the anti-Tn monoclonal antibody (mAb 83D4), which only reacted with the Tn^+ cell clone, while no 83D4 binding was detected in the parental (wt) and Tn^- cell lines (Figure 1A). This antibody was used since it binds both trimeric and dimeric Tn on cancer cells (Osinaga et al. 2000). Then, different lectins, recognizing carbohydrate structures present in O- or N-glycans were used (Figure 1B). Lectin recognition with the anti-Tn lectin from *Vicia villosa* (VVL) showed similar results (Figure 1C). Furthermore, lectin recognition with GalNAc-specific lectins, such as HPA, SBA and DBA confirmed the higher expression of terminal GalNAc structures in the selected Tn^+ cell line (Figure 1C). The proteins components present in the Tn^+ cell line were also detected by lectin blot using VVL, demonstrating a variety of components carrying the Tn antigen (Figure 1D).

We also analyzed the presence of other carbohydrate structures. As shown in Figure 1E, ECA (specific for terminal $\beta(1,4)$lactosamine) binding was similar for the three cell lines, while a decrease in PNA (with Gal$\beta(1,3)$GalNAc as its main ligand) recognition was detected in the Tn^+ cell line, indicating that core 1 (Gal$\beta(1–3)$GalNAc) synthesis may be inhibited due to Cosmc dysfunction. As PNA, MALII (a plant lectin specific for $\alpha(2–3)$-linked sialic acid) binding was significantly decreased in Tn^+ cells as compared with wt and Tn^- 4T1 cells (Figure G), indicating that the sialylation of Gal$\beta(1–3)$GalNAc was also disrupted. However, SNA reactivity (detecting αNeuAc(2,6)GalNAc), was decreased both in Tn^+ and Tn^- derived cell clones in comparison with wt cells (Figure 1G). We also analyzed the recognition by the mAb B72.3, first reported as specific for sialyl-Tn (Gold and Mattes 1988; Kjeldsen et al. 1988), and found a strong reactivity for Tn^+ cells but not for wt or Tn^- cells (Figure 1G). Further beyond O-glycans, no changes in WGA (GlcNAc in poly-N-acetyllactosamine repeats) or ConA (specific for mannose and glucose) were detected between Tn^+ or wt 4T1 cells. However, a small decrease in WGA binding in 4T1-Tn$^-$ cells was observed with respect to Tn^+ cells, while it was not detected in wt 4T1 cells (Figure 1F).

Tn antigen expression increases clonogenic and invasive capacity of 4T1 cells
In order to determine whether Tn antigen conferred growth advantage to 4T1 tumor cells, we analyzed cell proliferation, migration and invasion in vitro, as well as their capacity to form colonies. The three analyzed cell lines did not show any differences in their growth rate *in vitro* (Figure 2A). On the other hand, both Tn^+ and Tn^- 4T1 cells presented lower cell migration capacities, while higher clonogenic capacity, than the parental wt cell line (Figure 2B and C, respectively). Finally, the presence of the Tn antigen was associated with a higher invasion rate with respect to the wt and Tn- cell clones (Figure 2D). Thus, 4T1 cells expressing the Tn antigen display different alterations in their migration and invasive capacities, the latter being the one that distinguished them from the Tn^- and wt cells.

The Tn antigen confers TNBC cells with more aggressive and metastatic properties
To analyze the impact of Tn on tumor growth in vivo, 4T1-wt, Tn^+ and Tn^- cells were inoculated in the fourth right mammary fat pad of syngeneic mice and tumor growth was measured. Interestingly, tumors from Tn^+ cells were larger and at least three-times larger in volume than those from wt or Tn^- cells at day 28 post-injection (Figure 3A), an effect that was maintained when we analyzed tumor weight after mice sacrifice (Figure 3B). Furthermore, the presence of Tn antigen on tumors derived from the Tn^+ cell line was maintained in vivo, as shown by higher 83D4 recognition on CD45$^-$ cells from disaggregated tumors (Figure 3C). Since breast cancer aggressiveness is commonly associated with metastasis occurrence to distant organs, such as lungs, liver and bones, we analyzed lung micrometastases at day 28 after tumor cell implantation. As seen in Figure 3D, mice with tumors derived from 4T1-Tn$^+$ cells developed a significantly higher number of metastatic foci than those derived from mice inoculated with 4T1-wt cells. Lungs from mice inoculated with Tn^- cells or without tumors (naïve) did not develop metastases.
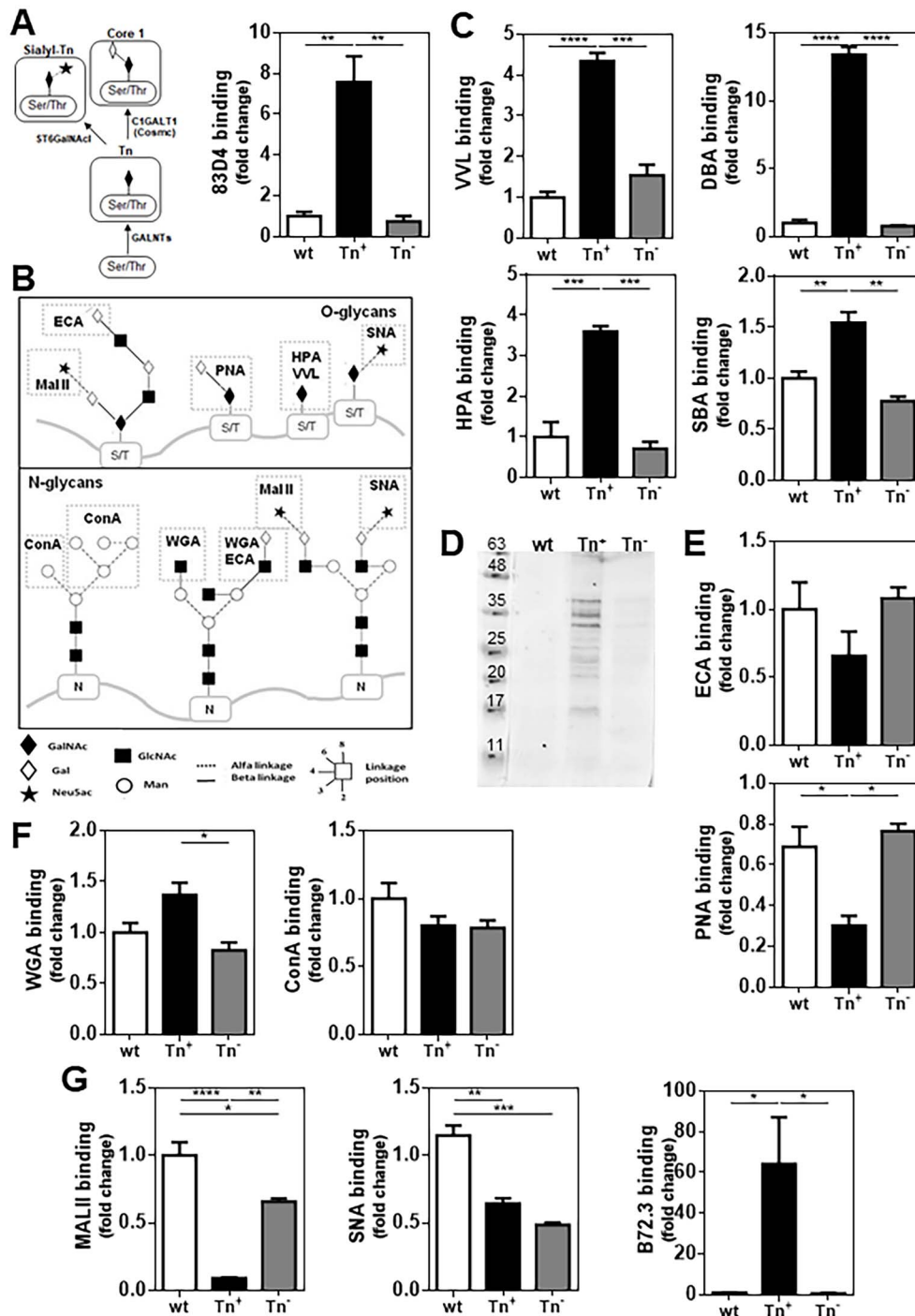
Fig. 1. *Cosmc*-KO 4T1 tumor cells express the Tn antigen. (A) Expression of Tn antigen on Tn+, Tn− and wt 4T1 tumor cells evaluated by flow cytometry with anti-Tn 83D4 antibody. Also, initial steps of mucin-type O-glycosylation are shown indicating glycosyltransferases such as GALNT (polypeptidyl-GalNAc-transferases), ST6GalNAcI ($\alpha a2,6$Sialyltransferase I) and C1GALT1 (core 1 Galactosyltransferase 1) (left). (B) Glycan motifs detected by lectins used in this study. (C) Recognition by terminal GalNAc-specific lectins: VVL, DBA, HPA and SBA, by flow cytometry. (D) VVL recognition of glycoproteins from Tn+, Tn− and wt 4T1 tumor cells by lectin blot. (E) Recognition by terminal Gal-specific lectins: ECA and PNA, by flow cytometry. (F) Recognition of N-glycan structures using WGA and ConA lectins by flow cytometry. (G) αNeuAc(2,3)Gal- and αNeuAc(2,6)GalNAc glycan structures analyzed by MALII and SNA lectins, respectively, analyzed by flow cytometry. Recognition by mAb B72.3 of Tn+, Tn− and wt 4T1 tumor cells was also evaluated by flow cytometry. Data are represented by the ratio between median fluorescence intensity obtained for Tn+ and Tn− cell lines relative to wt. Asterisks correspond to significant differences as follows: * $P < 0.05$, ** $P < 0.01$, *** $P < 0.001$, **** $P < 0.0001$ performed by one-way ANOVA followed by Tukey's test. Data are representative of three independent experiments.
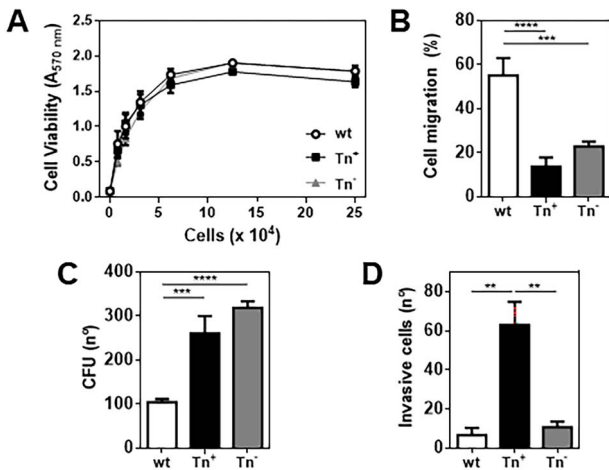
Fig. 2. Proliferation, clonogenicity, migration, and invasion capacity of obtained 4T1 cell lines. (A) Cell growth evaluated by viability with MTT. (B) Cell migration assessed by wound healing assay (C) Clonogenic capacity assessed by colony forming assay. (D) Cell invasion assay with collagen matrix. Asterisks correspond to significant differences as follows: ** $P < 0.01$, *** $P < 0.001$, **** $P < 0.0001$ performed by one-way ANOVA followed by Tukey's test. Data are representative of three independent experiments.

In order to correlate the 4T1 breast cancer model with clinical cases of advanced TNBC considering its metastatic potential, we evaluated the therapeutic impact of primary tumor resection at day 17, since, as we previously described, all animals develop lung metastasis at this time point when using wt 4T1 cell implantation (Kramer et al. 2015). Small tumors (4–8 mm diameter) were detected 12–14 days after orthotopic implantation of 4T1 cells and were surgically resected at day 17. Only 10% of tumor-bearing mice inoculated with the 4T1-Tn$^+$ cell line survived by day 75 after cell implantation, while 65 and 100% survival were observed at the same day for mice with tumors derived from 4T1-wt and Tn$^-$ cell lines, respectively (Figure 3E, Tn$^+$ vs. wt $P = 0.0146$: Tn$^+$ vs. Tn$^-$ $P < 0.0001$; wt vs. Tn$^-$ $P = 0.0024$). The autopsy of moribund mice revealed in all cases the presence of numerous macroscopic metastatic foci and a massive distortion of both lungs derived from Tn$^+$ tumor-bearing mice (Figure 3F). Of note, lungs derived from the parental 4T1 cell line presented few or none macroscopic metastatic foci, although organ distortion and color alterations were observed (Figure 3F). Therefore, the presence of the Tn antigen influence tumor growth and metastatic potential in the TNBC 4T1 mouse model.

Tn$^+$ cells generate tumors characterized by an increase in Foxp3$^+$ T cell infiltrate

To determine whether the presence of Tn affects the tumor immune microenvironment, we analyzed leukocyte infiltrates by flow cytometry in primary breast tumors at day 28 after cell inoculation. We focused on myeloid cells (Figure 4) and T lymphocytes (Figure 5), considering their role in immunosuppression (Kao et al. 2011; Glasner and Plitas 2021). In spite of the fact that no changes in the frequency of tumor-infiltrating CD45$^+$ cells were detected among the wt, Tn$^+$ and Tn$^-$ tumors, a higher proportion of CD11c$^+$ F4/80$^+$ immune cells was observed in Tn$^+$ tumors comparing to wt or Tn$^-$ tumors (Figure 4A). On the other hand, we observed

a higher frequency of both CD11b$^+$ MHCII$^-$ or CD11b$^+$ MHCII$^+$ immune cells in Tn$^+$ tumors than in wt and Tn$^-$ tumors, although this difference was only significant in the latter (Figure 4B, gate and plot a and b, respectively). Last, a decrease in the frequency of CD11b$^-$ MHCII$^+$ (that could account for lymphoid antigen presenting cells, such as B cells) was observed with respect to both wt and Tn$^-$ tumors. We further explored the Ly6G and Ly6C expression of these cells, in order to establish whether it could be a difference in the recruitment of potential myeloid suppressor cells in the tumors. The majority of CD11b$^+$ MHCII$^+$ expressed high levels of Ly6G and low levels of Ly6C (Figure 4C, plot a), while no differences on Ly6G and Ly6C expression were found on CD11b$^+$ MHCII$^+$ (Figure 4C, plot b) or CD11b$^-$ MHCII$^+$ cells (Figure 4C, plot c) between mice with different tumors. However, Tn$^-$ tumors presented a lower frequency of these cells when compared to wt and Tn$^+$ tumors. Altogether these results indicate that the presence of the Tn antigen is accompanied by a larger frequency of CD11c$^+$ F4/80$^+$ cells, which could account for antigen presenting cells.

On the other hand, the analysis of T cells in the tumor microenvironment revealed a decreased of CD3$^+$ T cells in Tn$^+$ tumors comparing both to wt and Tn$^-$ tumors, although this difference was not significant (Figure 5A). However, when we analyzed CD4$^+$ and CD8$^+$ T cells (Figure 5B and C, plots b and c, respectively), a lower frequency of these cells was observed on Tn$^+$ tumors than wt and Tn$^-$ tumors. Furthermore, CD4$^+$ T cells from Tn$^+$ tumors expressed higher levels of Foxp3 than those derived from wt and Tn$^-$ tumors (Figure 5C, plot d, left). However, CD8$^+$ T cells from all tumors expressed similar levels of FoxP3 (Figure 5C, plot d, right). Draining lymph nodes (DLN) from both Tn$^+$ and wt tumors presented lower frequencies of CD4$^+$ and CD8$^+$ T cells than those from Tn$^-$ tumors (Figure 5D, plots b and c, respectively). Nevertheless, a higher expression of Foxp3 was observed int CD4$^+$ T cells from DLN of Tn$^+$ tumors with respect to those from DLN of wt and Tn$^-$ tumors (Figure 5D, plots d), reflecting similar characteristics to cells recruited to Tn$^+$ tumors. In conclusion, these results demonstrate that the Tn antigen induces a recruitment of Foxp3 expressing CD4$^+$ T cells both in tumors and respective DLN in 4T1-inoculated mice.

Tn$^+$ tumor cells induce an immunoregulatory environment, both in tumors and metastatic lungs

To further characterize the immune response both systemically and in the metastatic organs, we first studied the capacity of splenocytes derived from tumor-bearing mice to produce different cytokines upon stimulation with anti-CD3 and anti-CD28 antibodies. Splenocytes derived from Tn$^+$ tumor-bearing mice produced lower levels of IFNγ and higher levels of IL-10 and IL-17 than mice with wt tumors (Figure 6A and B). A similar pattern was observed when comparing splenocytes from Tn$^+$ vs. Tn$^-$ tumor-bearing mice, although in this case, these latter produced slightly lower levels of IFNγ than those with Tn$^+$ tumors (Figure 6A and B). Of note, stimulated splenocytes from all tumor-bearing mice expressed lower levels of IFNγ than those from naïve mice. However, only stimulated splenocytes from Tn$^+$ tumor-bearing mice expressed higher levels of IL-10 and IL-17 than those from naïve mice.
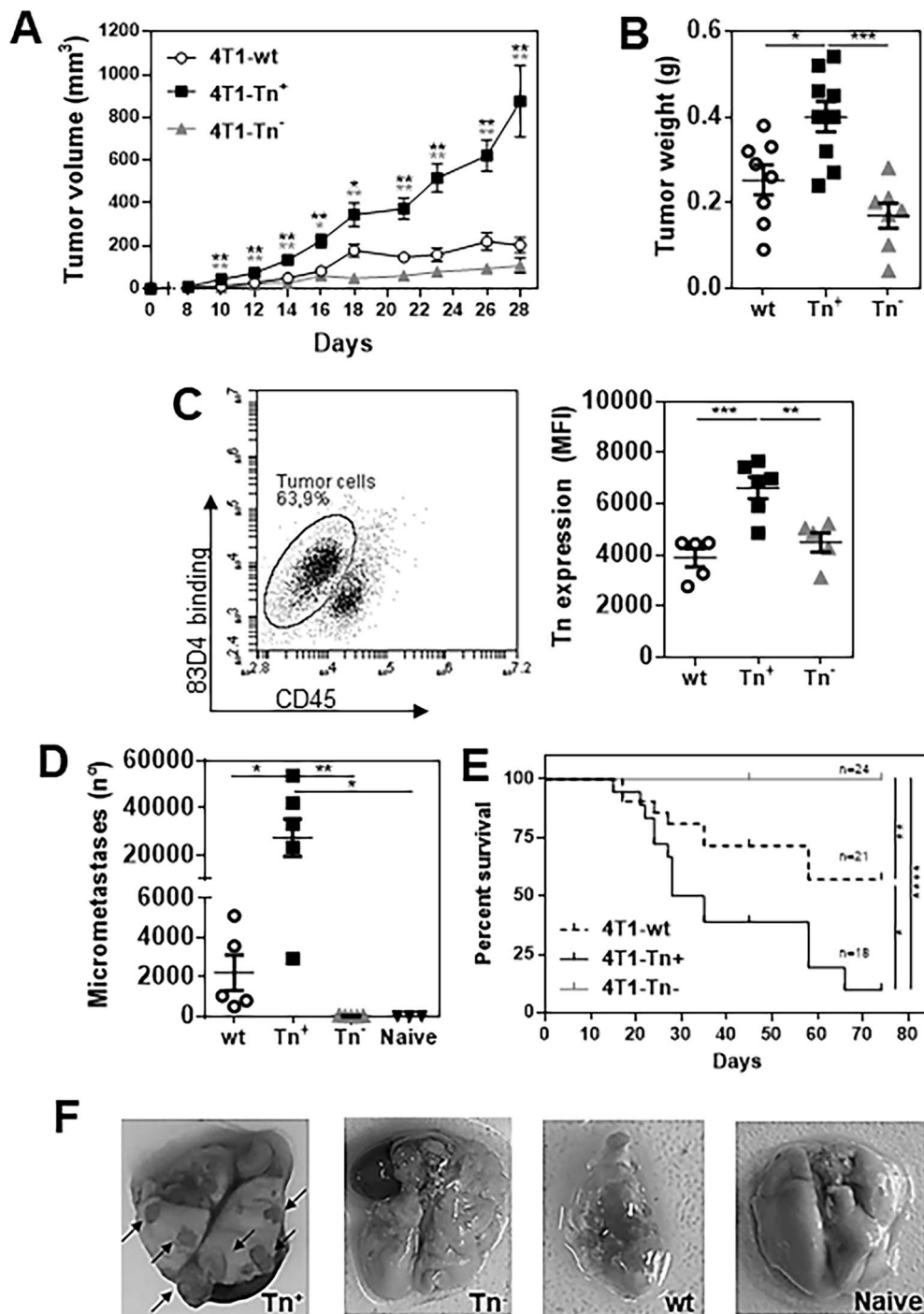
Fig. 3. Tn antigen expression favors primary tumor growth as well as lung metastases induced by 4T1 cell line. (A) Tumor growth evaluated on mice inoculated in the fourth right mammary fat pad with 70,000 4T1 cells (day 0). Five independent experiments are shown (Tn$^+$: $n = 43$; wt: $n = 41$; Tn$^-$: $n = 46$). (B) Tumor weight evaluated at day 28. (C) Expression of the Tn antigen in tumor cells (gated as CD45$^-$ cells) by flow cytometry using the anti-Tn mAb 83D4. (D) Breast cancer micrometastasis in the lungs. Tumor-bearing or naïve mice underwent tumor surgery at day 28, lungs were extracted and processed and the number of lung metastases was quantified. Lungs from naïve mice were used as a control. (D) Kaplan–Meier plot indicating animal survival of mice with primary tumor surgery at day 15. Three independent experiments are shown (Tn$^+$: $n = 18$; wt: $n = 24$; Tn$^-$:$n = 24$). (E) Lungs extracted from healthy control mouse (naïve) and from mice inoculated with Tn$^+$, Tn$^-$ or wt cell lines that underwent primary tumor surgical removal. Numerous metastatic nodules are observed in the lungs of mice inoculated with the 4T1-Tn$^+$ cell line. Asterisks correspond to significant differences as follows: * $P < 0.05$, ** $P < 0.01$, *** $P < 0.001$, **** $P < 0.0001$ performed by two-way ANOVA (A) or one way ANOVA followed by Tukey's test (B, C) or Log-rank (Mantel-Cox) test, Chi square (D). When not specified, data are representative of three independent experiments.
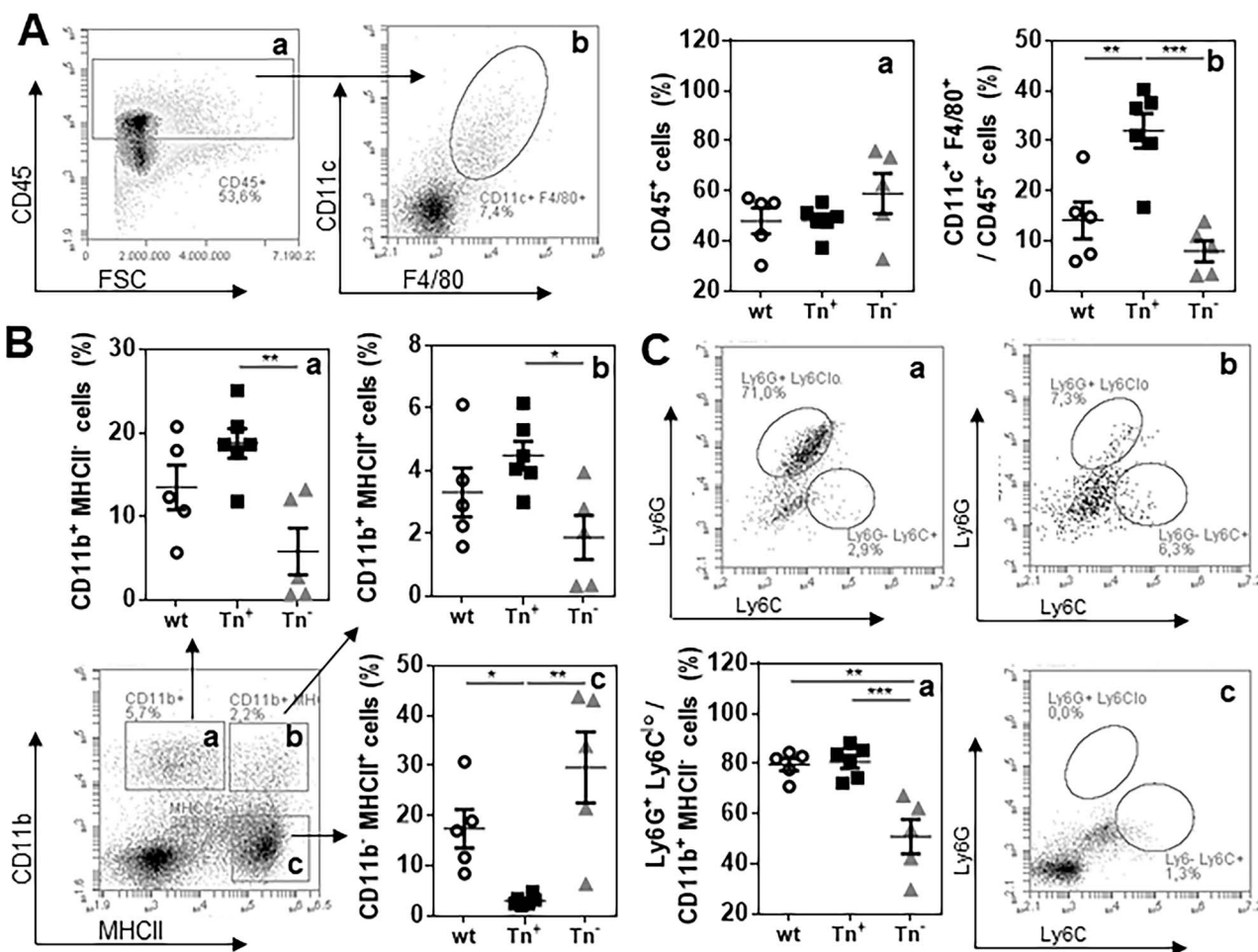
Fig. 4. Analyses of antigen presenting cells in tumor microenvironment. Tumor-bearing mice were sacrificed at day 28, tumors were removed and analyzed by flow cytometry. (A) Frequency of CD45$^+$ cells and CD11c$^+$ F4/80$^+$ cells infiltrating the tumor. (B) Frequency of CD11b$^+$ MHCII$^-$, CD11b$^+$ MHCII$^+$ and CD11b$^-$ MHCII$^+$ tumor infiltrating immune cells. (C) Expression of Ly6G and Ly6C on CD11b$^+$ MHCII$^-$, CD11b$^+$ MHCII$^+$ and CD11b$^-$ MHCII$^+$ tumor infiltrating immune cells. Asterisks correspond to significant differences as follows: * $P < 0.05$, ** $P < 0.01$, *** $P < 0.001$, performed by one-way ANOVA followed by Tukey's test. Data are representative of three independent experiments.

We also analyzed the production of IFNγ, IL-10 and IL-17 in lungs derived from tumor-bearing mice. To this end, we collected the supernatant of disaggregated lungs. We observed a higher expression of IL-10 by lungs derived from Tn$^+$ tumor-bearing mice than by those derived from naïve mice, while no differences were observed for IL-10 produced in mice with wt and Tn$^-$ tumors (Figure 6C and D). Altogether, these results indicate that the presence of the Tn antigen is related with increased levels of IL-10 produced by the spleen and the lungs in tumor-bearing mice.

The Tn antigen induces higher production of ROS/RNS by tumor cells

Last, we analyzed the capacity of tumor cells to produce ROS/RNS by flow cytometry. As seen in Figure 7, both Tn$^+$ cell lines (Figure 7A) and Tn$^+$ tumors (Figure 7B) produced higher levels of ROS/RNS than wt and Tn$^-$ 4T1 cell lines. Since ROS and RNS can inhibit T cell proliferation (Halasi et al. 2013; Garcia-Ortiz and Serrador 2018), and considering that splenocytes from Tn$^+$ tumor-bearing mice were not able to produce IFNγ upon CD3/CD28 stimulation (Figure 6A), we wondered whether the production of ROS by Tn$^+$ tumor cells might inhibit production of IFNγ by stimulated naïve

splenocytes. To address this, CD3/CD28-stimulated naïve splenocytes were incubated with supernatants from wt, Tn$^+$ and Tn$^-$ tumors, in the presence or absence of NAC, a ROS scavenger. The supernatants from the three types of breast tumors completely abrogated the production of IFNγ by stimulated splenocytes. However, culturing them with NAC lead to a significant increase of IFNγ production in the presence of wt or Tn$^-$, but not Tn$^+$, tumor-derived supernatants (Figure 7C). Of note, not detectable levels of IL-10 were found in splenocyte culture media (not shown). Altogether, these results suggest that Tn$^+$ tumor cells produce higher ROS/RNS levels, and that ROS derived from Tn$^+$ tumors is not implicated in the suppression of IFNγ production by stimulated splenocytes.

Discussion

In the present study, we demonstrate that the induction of Tn antigen expression promotes lung metastases in an orthotopic TNBC murine model. We also show that both primary tumors and metastatic lungs are characterized by an immunoregulatory environment. Altered protein glycosylation is a hallmark of carcinomas and one of the most
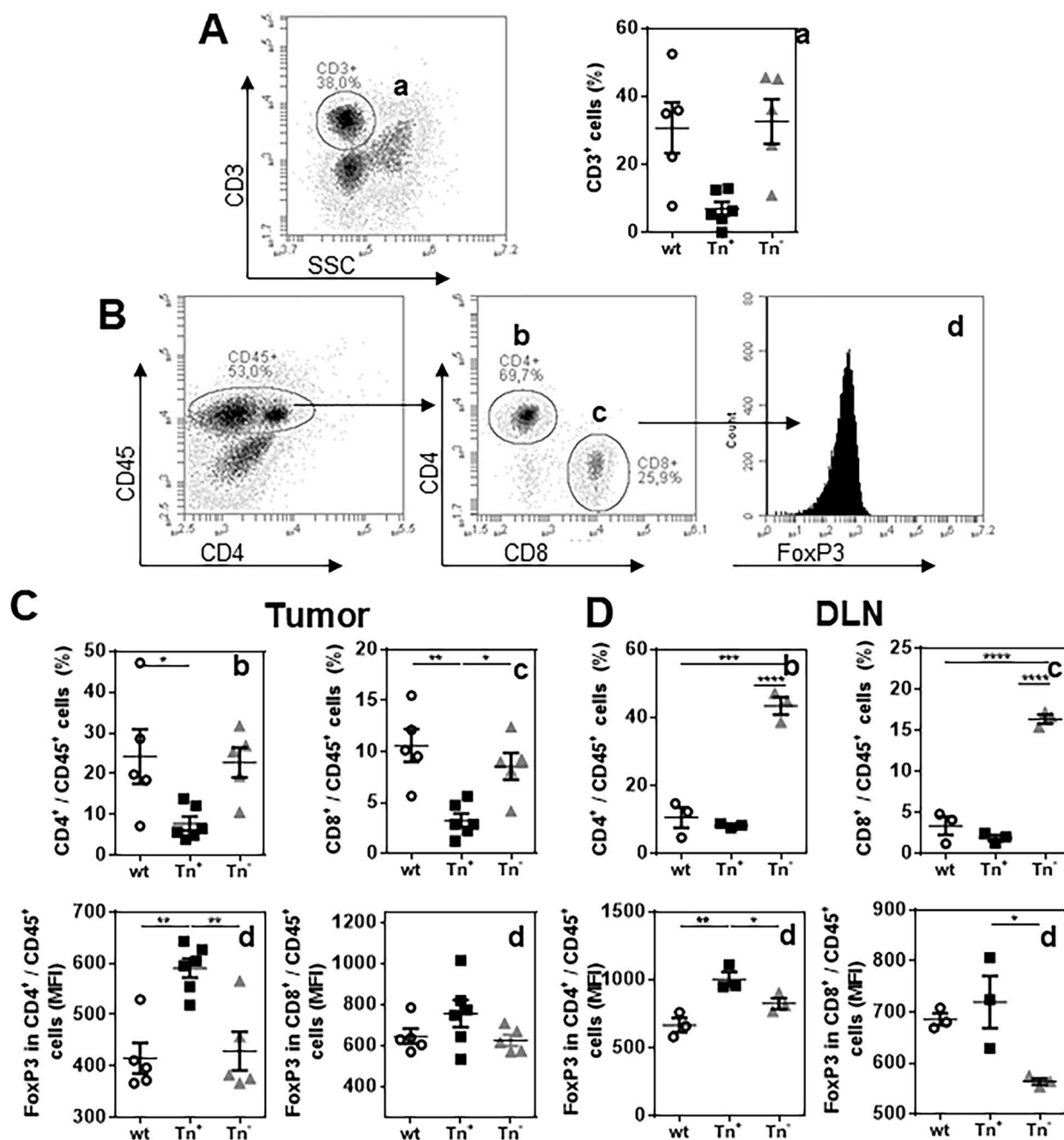
Fig. 5. The Tn antigen induces the recruitment of Foxp3-expressing CD4+ T cells both in the tumor and draining lymph nodes. Tumor-bearing mice were sacrificed at day 28, tumors and DLN were removed and analyzed by flow cytometry. (A) Frequency of CD3+ T cells infiltrating the tumor. (B) Gate strategy to select CD4+ and CD8+ T cells expressing Foxp3. (C) Frequency of CD4+ or CD8+ T cells infiltrating the tumor and evaluation of Foxp3 expression. (D) Frequency of CD4+ or CD8+ T cells in DLN and evaluation of Foxp3 expression. Asterisks correspond to significant differences as follows: * $P < 0.05$, ** $P < 0.01$, *** $P < 0.001$, **** $P < 0.0001$ performed by one-way ANOVA followed by Tukey's test. Data are representative of three independent experiments.

common cancer-associated changes in glycosylation is the truncation of O-linked carbohydrate chains as a consequence of the impairment of the normal elongation of O-glycans (Pinho and Reis 2015), leading to Tn antigen expression, among other structures (Ju et al. 2008; Kudelka et al. 2015). To study the metastatic role of the Tn antigen in TNBC, we used the SimpleCell strategy (Steentoft et al. 2013), consisting in genetically engineering the *Cosmc* gene in the

4T1 tumor cell line, the molecular chaperone for T-synthase that is essential for Tn antigen elongation. The expression of the Tn antigen in Tn+ 4T1 cells was confirmed by cell glycophenotyping demonstrating a clear over expression of this structure in agreement with GalNAc-binding lectins and a decrease of PNA recognition in comparison with parental wt and Tn− cell lines. However, the obtained Tn− cell clone, as the Tn+ one, presented a decrease in SNA-
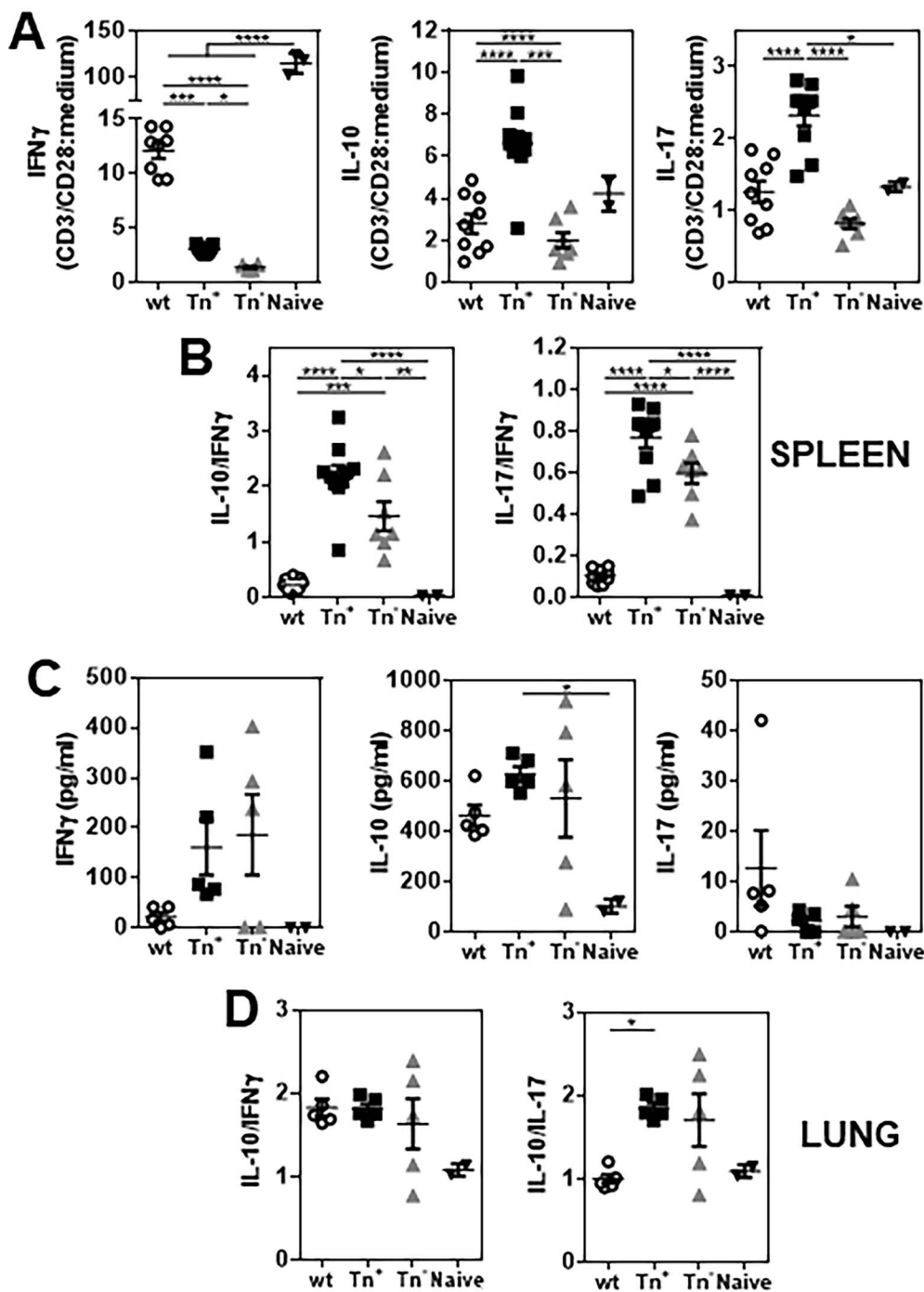
Fig. 6. Expression of Tn antigen on tumors favors systemic production of IL-10 both in the tumor and in the metastatic microenvironment. Tumor-bearing mice were sacrificed at day 28, spleens and lungs were removed and cytokine production was analyzed by specific sandwich ELISA. Naïve mice were used as control. (A) Splenocytes (0.5×10^6/well) from Tn$^+$, Tn$^-$ or wt tumor-bearing mice were cultured in the presence or absence of CD3/CD28 (1 μg/mL) for 5 days at 37°C and 5% CO_2. IFNγ, IL-10 and IL-17 levels were quantified on culture supernatants. Results are shown as the ratio of the stimulated with respect to the medium (control) conditions. (B) Levels of IL-10 or IL-17 in relation to IFNγ levels. (C) Lungs from Tn$^+$, Tn$^-$ or wt tumor-bearing mice were disaggregated and cultured for 2 h in complete medium at 37°C. IFNγ, IL-10 and IL-17 levels were quantified on culture supernatants. (D) Levels of IL-10 in relation to IFNγ or IL-17 levels. Asterisks correspond to significant differences as follows: * $P < 0.05$, ** $P < 0.01$, *** $P < 0.001$, **** $P < 0.0001$ performed by one-way ANOVA followed by Tukey's test. Data are representative of three independent experiments.

binding, indicating that, although it has undergone the same transformation process, the sialylation process is altered with regard to the parental cell line, indicating a decrease in NeuAcα(2–6)Gal or GalNAc residues. In this regard, a

glycosyltransferase enzymatic dysregulation could be the result of signaling pathways potentially modulated by aberrant O-glycosylation, as demonstrated recently in gastric cancer cells (Freitas et al. 2019). Importantly, a strong
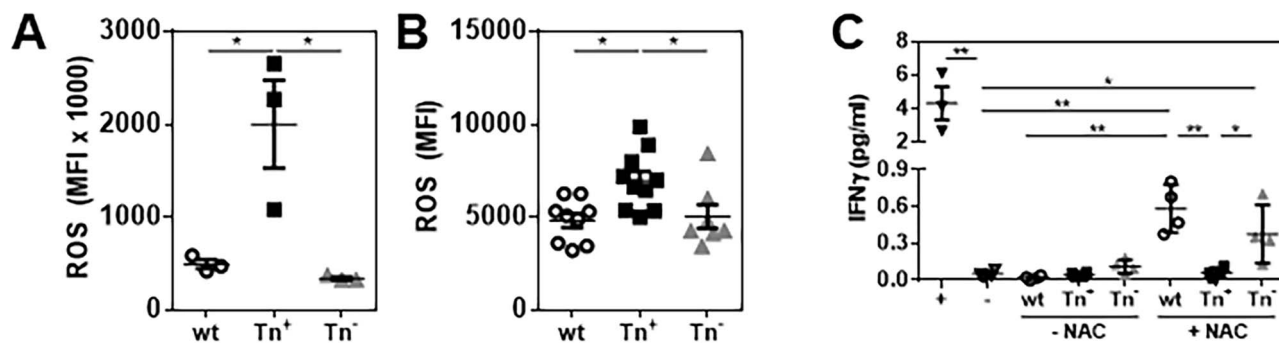
Fig. 7. Tn$^+$ tumor cells produce high ROS or RNS levels. (A) Tn$^+$, Tn$^-$ and wt 4T1 tumor cells were cultured and stained with an ROS/RNS specific probe and evaluated by flow cytometry. (B) Tn$^+$, Tn$^-$ and wt 4T1 tumors from 4T1-inoculated mice were stained with an ROS/RNS specific probe and analyzed by flow cytometry on CD45$^-$ cells. (C) Splenocytes from naïve mice were cultured in the presence (+) or absence (−) of CD3/CD28 (1 μg/mL) for 5 days at 37°C and 5% CO$_2$. Supernatants from wt, Tn + or Tn$^-$ disaggregated tumors were incubated with stimulated splenocytes in the presence or absence of 5 mM NAC, an ROS scavenger. IFNγ levels were quantified on culture supernatants. Asterisks correspond to significant differences as follows: * $P < 0.05$, ** $P < 0.01$, performed by Student unpaired t test.

reactivity for Tn$^+$ cells was found by the mAb B72.3. This antibody was first reported by its high sialyl-Tn specificity. (Gold and Mattes 1988; Kjeldsen et al. 1988) However, these results must be carefully interpreted since later, a cross reactivity for the Tn antigen was described in many works (Colcher et al. 1981; Reddish et al. 1997; Julien et al. 2012; Persson et al. 2017; Prendergast et al. 2017). Thus, the high reactivity of this antibody for Tn$^+$ cells would be due to its interaction with Tn-expressing glycoproteins rather than to sialyl-Tn.

Tn antigen expression has been associated to neoplastic progression, by enhancing cell proliferation, decreasing apoptosis and increasing adhesion and migratory capacities (Radhakrishnan et al. 2014; Hofmann et al. 2015; Dong et al. 2018). In the same line, in our model, Tn$^+$ tumor cells presented a higher capacity to invade a collagen-rich membrane in vitro. Furthermore, recent reports demonstrated that Tn expression associates with enhanced tumor growth and the recruitment of potentially immunoregulatory cells (Cornelissen et al. 2020; Dusoswa et al. 2020). The observation that the expression of Tn in primary tumors was associated with lymph node involvement (Kawaguchi et al. 2006; Konska et al. 2006) and even with invasion of lymphatic vessels within the primary tumor (Kawaguchi et al. 2006) suggested a role of this antigen in the metastatic process. However, no studies have been reported about the role of Tn antigen in fostering metastasis driven by TNBC cells. In this line, our work provides evidence, for the first time, that the Tn antigen in TNBC cells favors lung metastases, in association with systemic and local immunosuppression, both at the primary tumor and at the metastatic site. Unexpectedly, the selected Tn$^-$ cell clone, presented a lower metastatic capacity than the parental wt cell line, both evidenced by lower lung micrometastasis detection and mice survival. This less malignant phenotype of the Tn$^-$ cell line might be explained by the significant reduction in the expression of sialic acids attached to terminal galactose in α-2,6 and α-2,3 linkage identified by SNA binding with respect to the wt cell line. The lack of Tn and the reduction in sialyl-Tn expression in this cell line may account for its reduced metastatic potential and its greater survival rate. Furthermore, our results suggest that far beyond the role of SNA-ligands between the wt ant Tn$^-$ cell lines, a mutation in *Cosmc* compensates these possible effects in a way that makes the Tn$^+$ even more aggressive than the parental cell line. This is in accordance with other works that reported that truncated O-glycans expression leads to a more aggressive phenotype and promotes metastasis potential (Radhakrishnan et al. 2014; Chugh et al. 2018; Freitas et al. 2019; da Costa et al. 2021). Thus, we have obtained two different sublines derived from the TNBC 4T1 cell line, with different metastatic potential, that might represent a great research tool, for example to study diverse therapeutic strategies, as it happens with other mouse cancer models (Danciu et al. 2015).

Primary tumors and DLN were characterized by a higher expression of FoxP3 in CD4$^+$ T cells, suggesting a connection between the Tn antigen and the generation of Tregs. Furthermore, stimulated splenocytes and lungs produced higher levels of IL-10 probably favoring the development of metastases. Tn$^+$ tumors were also characterized by a recruitment of CD11c$^+$ F4/80$^+$ cells that could account for antigen presenting cells. Indeed, these cells might recognize the Tn antigen through the C-type lectin receptor Macrophage Galactose-type Lectin (MGL; CD301) (Saeland et al. 2007; Beatson et al. 2015) and might induce the differentiation of naïve T cells to Tregs (da Costa et al. 2021). Indeed, several reports demonstrated that MGL-expressing myeloid cells can induce Treg differentiation (Li et al. 2012) and suppression of T cell activation (van Vliet et al. 2006). Tn$^+$-derived splenocytes also produced higher levels of IL-17 upon polyclonal stimulation, although they were lower than those of IL-10. Interestingly, IL-17 can play a detrimental role in the development of an effective anti-tumor T cell response (Dadaglio et al. 2020). Even though strong Th1-type responses favor tumor control, the simultaneous activation of Th17 cells may redirect or curtail tumor-specific immunity through a mechanism involving neutrophils (Dadaglio et al. 2020). In this regard, it might be interesting to study whether the production of IL-10 and IL-17 depends on MGL$^+$ myeloid cells.

It is worth noting that the identity or the function of the Tn$^+$ molecules still remain to be determined. Other reports have shown the Tn antigen-driven metastases could be consequence of cancer cell adhesion to the endothelial lining of vessels (Bapu et al. 2016), enhancing the activity of matrix metalloproteinase 14 in liver cancer (Nguyen et al. 2017) or promoting the epithelial and mesenchymal transition (EMT) of tumor cells in a process where transforming growth factor beta (TGFβ1) or its receptor were involved (Freire-de-Lima et al. 2011). Other works have identified Tn on MUC1

(Park et al. 2010) or osteopontin (Minai-Tehrani et al. 2013) as key actors that enhance breast cancer progression, although their role in the metastatic process has not yet been proved.

It has been demonstrated that high expression of ROS by both tumors and/or other cells within the tumor microenvironment suppresses T-cell proliferation and anti-tumor immune responses (Halasi et al. 2013). Moreover, the high expression of ROS and oxidative stress in the tumor environment can induce a stronger immunosuppression by Tregs (Maj et al. 2017). In our work, we could demonstrate that ROS produced by wt and Tn$^-$ is, at least in part, involved in the inhibition of IFNγ production by stimulated splenocytes. However, we could not confirm this hypothesis with ROS produced by Tn$^+$ tumors, meaning that RNS or other tumor-derived soluble molecules might be involved in this process. In conclusion, our work demonstrates that the Tn antigen induces both TNBC growth and lung metastases and immunosuppression. In this sense, blocking the Tn antigen could constitute a novel therapeutic strategy to dampen TNBC-derived metastases.

Materials and methods
Cell line engineering
The murine TNBC cell line 4T1 (Gupta et al. 2021; Zhang et al. 2021) was obtained from ATCC and cultured in DMEM with glutamine (Capricorn, Germany or Gibco, USA) supplemented with 10% inactivated fetal bovine serum (Capricorn, Germany) and antibiotic-antimycotic (Thermo Fisher) at a final concentration of 100 units/mL of penicillin, 100 μg/mL of streptomycin, and 0.25 μg/mL of Gibco Amphotericin B (complete culture medium). Cells were maintained at 37°C in a humidified atmosphere of 5% CO$_2$. When needed, cells were harvested by washing with phosphate-buffered saline (PBS) pH 7.4 and incubation with a *trypsin* (0.1%)/EDTA (0.04%) solution.

Defects in the enzymes that participate in the O-glycosylation process, such as the Core 1 β3-galactosyltransferase and Core 1 β3-galactosyltransferase Specific Molecular Chaperone (Cosmc) (Ju et al. 2008; Yoo et al. 2008) lead to the expression of the Tn antigen. Thus, Tn$^+$ 4T1 cells were generated by targeting the *Cosmc* gene using Crispr/Cas9 precise gene editing. Transfection of 4T1 cells was carried out by CRISPR guide targeted to *Cosmc* exon 2 170 s (GATATCTCGAAAATTTCAG) cloned in pBS-U6sg plasmid (Tacgene, France) and GFP-tagged Cas9-PBKS (Addgene). About, 4T1 cells were seeded in 24 well plates (2 x 10^5 cells per well) and after one day 0.5 μg of gRNA was co-transfected with 0.5 μg of GFP-tagged Cas9-PBKS using Lipofectamine 3000 (Invitrogen). Cells were harvested after 48 h, and single-sorted into 96 well plates for GFP expression by FACS (BD FACSAria™ Fusion). The expression of Tn antigen in the obtained clones was verified by staining with the anti-Tn mAb 83D4 (Osinaga et al. 2000) and the mutations in *Cosmc* in the selected clones were further verified by Sanger sequencing using the following primers: Cosmc-F: 5'-ATCACTATGCTAGGCCACATTAGGATTGGA-3' and Cosmc-R: 5'-GGAGGTAAGAAAACCAATGCATCATTGAA AA-3'. An insertion of 1 T in one allele ($^+$) and a deletion of 1 T ([T]) in the other were found in the following positions: 5'- GATATCTCGAAAATT[T]$^+$TCAG-3' in the Tn$^+$ cell line.

A Tn$^-$ clone was also selected for further characterization according to Tn expression.

Lectin and antibody recognition of tumor cells by flow cytometry
Wild type (wt) Tn$^-$ and Tn$^+$ 4T1 tumor cells were harvested and washed with PBS. They were stained with anti-Tn antibody 83D4 (Osinaga et al. 2000) or the following lectins: *Helix pomatia* lectin (HPA, GalNAc, Tn antigen, 1 μg/μl), Isolectine B4 of *V. villosa* lectin (VVL. GalNAc, Tn antigen, 2 μg/μl), *Arachis hypogaea* lectin (PNA: βGal(1,3)GalNAc, 1 μg/μl), *Erythrina cristagali* lectin (ECA: βGal(1–4)GlcNAc, 1 μg/μl), *Soybean agglutinin* (SBA: GalNAc, Tn antigen, 5 μg/μl), *Sacumbus Nigra* lectin (SNA: αNeuAc(2,6)Gal, 5 μg/μl), *Maackia amurensis* II lectin (Mal II: αNeuAc(2,3)Gal, 1 μg/μl), *Triticum vulgaris* lectin (WGA: (GlcNAc)$_2$, 1 μg/μl), *Canavalia ensiformis* (ConA: αMan>αGlc, 1 μg/μl) in PBS containing 2% FBS 0,02% Na$_3$N (FACS buffer). Cells were washed twice and incubated with APC-conjugated streptavidin (for lectins) or a FITC-conjugated anti-mouse IgM (for 83D4 anti-Tn mAb).

Cell viability
Tn$^+$, Tn$^-$ and wt 4T1 cells were harvested and plated in triplicates on 96-well plates at half-serial dilutions starting from 250.000 cells/well (100 μl) and incubated at 37°C for 24 h. 3-(4,5 dimethyl-2 thiazolyl)-2,5 diphenyl-2H tetrazolium (MTT, Sigma-Aldrich, USA) bromide solution was added to each well at a final concentration of 0.5 mg/ml and incubated for 4 h at 37°C. The formazan crystals were dissolved with 100 μl of 10% SDS in 0.01 M HCl and absorbance was measured at 570 nm with a plate spectrophotometer after overnight incubation at 37°C.

Colony forming assay
Tn$^+$, Tn$^-$ and wt 4T1 cells were harvested and plated in 100-mm dishes at a final concentration of 500 cells/dish and incubated at 37°C for 10 days. Then, growth medium was removed and cells were stained with 0.05% crystal violet, 1% formaldehyde and 1% methanol in PBS for 20 min at room temperature. Colony formation units were counted manually.

Cell migration by wound healing
Tn$^+$, Tn$^-$ and wt 4T1 cells were harvested and plated in 6-well plates (5 × 10^5 cells/well). Twenty-four hours before making the wound, the culture media was changed from 10 to 0.5% of FBS. When they reached confluence, a wound was done to the monolayer with a 200-μl tip. Cells were washed twice with PBS to eliminate cell debris, and then cultured in 0.5% FBS growth medium for 24 h. Photos were taken at 0 and 24 h in epifluorescent microscope Leica TCS SP5 II and analyzed with Image J.

Cell invasion
Corning transwell with 8-μm pore polycarbonate membrane cell culture inserts were used in 24-well plates. About, 7100 μl of a solution of 0.5 mg/ml of collagen in 20 mM HEPES, 26 mM NaHCO$_3$, 5 mM NaOH was used in each transwell and left to gel at 37°C for 2 h. About, 500 μl of complete growth medium (supplemented with 10% FBS) was added to the bottom of the well. wt, Tn$^-$ and Tn$^+$ 4T1 cells were harvested and 2x10^5 cells were seeded into each transwell in

FBS-depleted growth medium and incubated at 37°C for 48 h. Transwells were washed with PBS twice and cells attached to the top side of the transwell were cleaned using a cotton swab. Cells in the bottom layer of the transwell were stained with a solution of 0.05% w/v crystal violet, 1% formaldehyde and 1% methanol in PBS for 20 min at room temperature. Then, transwells were washed with water, and cells were counted with an optical microscope.

Tumor growth in vivo

Six-to eight-week-old female BALB/c mice were purchased from DILAVE Laboratories (Uruguay), or URBE (Facultad de Medicina, UdelaR, Uruguay). Animals were kept in the animal house (URBE) with water and food supplied ad libitum. Mouse handling and experiments were carried out in accordance with strict guidelines from the National Committee on Animal Research (CNEA, Uruguay). All procedures involving animals were approved by the Universidad de la República's Committee on Animal Research (CHEA Protocols N° 070153–000732-17). Cells were harvested at 60–70% confluence, washed, counted and inoculated in the 4th right mammary fat pad with 70 000 4T1 cells resuspended in 50 μl of phosphate saline buffer (PBS). Fifteen days after cell implantation, 100% mice showed palpable tumors. Tumor size was measured from day of first appearance every 2–3 days, and tumor volume was calculated as $V = 4/3.\pi.(r_1.r_2^2)$, being r_1 the largest ratio. Animals were sacrificed at day 28 and tumors were weighted and processed for analyses. At least eight mice were used per group in each study.

Lung micrometastasis

Lung micrometastases were quantified by a standard clonogenic assay due to the inherent resistance of 4T1 cells to 6-thioguanine treatment (Aslakson and Miller 1992; Pulaski and Ostrand-Rosenberg 1998; Kramer et al. 2015). Mice were sacrificed 28 days after tumor cells implantation, lungs were isolated and finely minced with sterile scissors and digested in a 5 ml of PBS solution containing 20 mg Collagenase type IV (Gibco, USA) and 50 μg DNAse I (Sigma-Aldrich) for 1 h at 37°C on a rotating wheel. After incubation, 5 mM EDTA was added to stop the enzymatic reaction and the tissue was homogenized by pipetting several times. The homogenate was washed in 10 ml PBS, and samples were filtered through a 70-μm Falcon cell strainer (BD Biosciences) to obtain a clear solution. This solution was washed twice in DMEM by 1500 rpm centrifugation at 4°C. The cell pellet was resuspended and serially diluted in 6-well tissue culture plates containing complete culture medium supplemented with 60 μM 6-thioguanine (Sigma Aldrich). Tumor cells formed foci within 10–14 days. Cell clones were fixed with PFA 4% and stained with 0.03% methylene blue solution for macroscopic counting. At least six mice were used per group in each study.

Mice survival

Death of tumor-bearing mice due to lung metastases was determined on mice without primary breast tumors. Surgical removal of tumors was performed essentially as described previously (Pulaski et al. 2000; Pulaski and Ostrand-Rosenberg 2001; Kramer et al. 2015) with the proximal draining lymph node (DLN) also removed along with the adjoining abdominal fat at day 15. Wounds were closed using a sterile 19 mm 3/8 nylon monofilament suture (HAD, China). Paracetamol (1 mg/ml) dissolved in drinking water was given to animals for 24 h to aid the post-operatory recovery. Survival was monitored regularly, and animals were euthanized if found moribund during the observation period. Dead mice were autopsied to check for the presence of lung metastasis. At least six mice were used per group in each study.

Analyses of tumor microenvironment by flow cytometry

Tumors were disaggregated and incubated with Collagenase Type IV (100 U/ml, Gibco, USA). Then, red blood cells were lysed and tumor-derived cells were washed with FACS buffer, counted and incubated (0.2 × 10⁶ cells/well) with anti-CD45 (104), -F4/80 (BM8), -CD11c (N418), -CD4 (GK1.5), -CD8α (53.6–7), -CD3 (17A2), CD11b (M1/70), −Ly6G (RB6-8C5), -Ly6C (HK1.4), -I-A/I-E (M5/114.4.2) in FACS buffer for 30 min at 4°C. When stained with anti-Tn antibody 83D4 cells were pre-incubated with stripping buffer (0.1 M glycine, 4 g/L NaCl pH 2) for 30 min at 37°C. For intracellular staining, the Intracellular Staining Perm Wash Buffer and Fixation Buffer (BioLegend, USA) was used according to manufacturer protocol, and anti-FoxP3 (FJK-16 s) was incubated for 1 h at RT. Cells were then washed and measured in an Accuri flow cytometer and analyzed with BD Accuri C6 Plus software. DLNs were disaggregated in PBS and analyzed by flow cytometry using the same strategy.

Reactive oxygen and nitrogen species determination

Reactive oxygen/nitrogen species (ROS/RNS) produced by both tumor cell lines and tumors were determined with 2′,7′-Dichlorofluorescein diacetate (DCFDA) probe, a fluorogenic dye that is oxidized into the fluorescent 2′,7′-Dichlorofluorescein. Briefly, cells were incubated in PBS for 30 min at 37°C with DCFDA by flow cytometry. Then, they were washed with FACS buffer and fluorescence was measured in an Accuri flow cytometer and analyzed with BD Accuri C6 Plus software. A similar strategy was used to analyze ROS/RNS in tumors. In this case, tumor cells were first incubated with anti-CD45 antibody and gated as CD45⁻ cells.

Analyses of splenocyte proliferation

Splenocytes from tumor-bearing mice (1 × 10⁶ cell/well) were cultured in RPMI-1640 with glutamine (Capricorn, Gibco, Germany) complete medium containing 10% FBS, 50 μM 2-mercaptoethanol, 100 U/mL penicillin, 0.1 mg/mL streptomycin in the presence or absence of CD3/CD28 (1 μg/mL) for 5 days at 37°C and 5% CO_2. IFNγ, IL-10 and IL-17 levels were quantified on culture supernatants by specific sandwich ELISA (BD Biosciences or Biolegend) according to the manufacturer's instructions. IFNγ, IL-10 and IL-17 levels were also quantified on culture media from disaggregated lung supernatants. To evaluate ROS effect on splenocyte proliferation, N-acetyl-l-Cystein (NAC), an ROS scavenger (Halasi et al. 2013), was used. Cells from naïve mice were cultured in RPMI complete culture medium in the presence or absence of CD3/CD28 (1 μg/mL), 5 mM NAC and Tn⁺, Tn⁻ or wt-tumor derived culture supernatants for 5 days at 37°C and 5% CO_2. IFNγ levels were quantified by specific sandwich ELISA as described above.

Statistical analyses

Statistical analyses were performed with Prism software (GraphPad Prism 6.01). The Student unpaired t test, one way ANOVA or two way ANOVA were used to determine, according the experiment, the significance of the differences. Survival curves obtained by the Kaplan-Meyer method were statistically analyzed using the Log-rank test. Asterisks indicate statistically significant differences with $*P < 0.05$; $**P < 0.01$; $***P < 0.001$. Data are representative of at least two individual experiments.

Funding

Acknowledgements

Data Availability statement

Data are available upon request to the authors.

Competing interests

The authors declare that they have no conflict of interest.

References

Abramson VG, Mayer IA. 2014. Molecular heterogeneity of triple negative breast cancer. *Curr Breast Cancer Rep*. **6**:154–158.

Aslakson CJ, Miller FR. 1992. Selective events in the metastatic process defined by analysis of the sequential dissemination of subpopulations of a mouse mammary tumor. *Cancer Res*. **52**:1399–1405.

Bapu D, Runions J, Kadhim M, Brooks SA. 2016. N-acetylgalactosamine glycans function in cancer cell adhesion to endothelial cells: A role for truncated O-glycans in metastatic mechanisms. *Cancer Lett*. **375**:367–374.

Beatson R, Maurstad G, Picco G, Arulappu A, Coleman J, Wandell HH, Clausen H, Mandel U, Taylor-Papadimitriou J, Sletmoen M *et al.* 2015. The breast cancer-associated Glycoforms of MUC1, MUC1-Tn and sialyl-Tn, are expressed in COSMC wild-type cells and bind the C-type lectin MGL. *PLoS One*. **10**:1–21.

Chia J, Goh G, Bard F. 2016. Short O-GalNAc glycans: Regulation and role in tumor development and clinical perspectives. *Biochim Biophys Acta*. **1860**:1623–1639.

Chugh S, Barkeer S, Rachagani S, Nimmakayala RK, Perumal N, Pothuraju R, Atri P, Mahapatra S, Thapa I, Talmon GA *et al.* 2018. Disruption of C1galt1 gene promotes development and metastasis of pancreatic adenocarcinomas in mice. *Gastroenterology*. **155**:1608–1624.

Colcher D, Hand PH, Nuti M, Schlom J. 1981. A spectrum of monoclonal antibodies reactive with human mammary tumor cells. *Proc Natl Acad Sci U S A*. **78**:3199–3203.

Cornelissen LAM, Blanas A, Zaal A, van der Horst JC, Kruijssen LJW, O'Toole T, van Kooyk Y, van Vliet SJ. 2020. Tn antigen expression contributes to an immune suppressive microenvironment and drives tumor growth in colorectal cancer. *Front Oncol*. **10**:1622.

da Costa V, van Vliet S, Carasi P, Frigerio S, García P, Croci D, Festari M, Costa M, Landeira M, Rodríguez-Zraquia SA *et al.* 2021. The Tn antigen promotes lung tumor growth by fostering immunosuppression and angiogenesis via interaction with macrophage galactose-type lectin 2 (MGL2). *Cancer Lett*. 72–81.

Dadaglio G, Fayolle C, Oberkampf M, Tang A, Rudilla F, Couillin I, Torheim EA, Rosenbaum P, Leclerc C. 2020. IL-17 suppresses the therapeutic activity of cancer vaccines through the inhibition of CD8(+) T-cell responses. *Onco Targets Ther*. **9**:1758606.

Danciu C, Oprean C, Coricovac DE, Andreea C, Cimpean A, Radeke H, Soica C, Dehelean C. 2015. Behaviour of four different B16 murine melanoma cell sublines: C57BL/6J skin. *Int J Exp Pathol*. **96**:73–80.

Dong X, Jiang Y, Liu J, Liu Z, Gao T, An G, Wen T. 2018. T-synthase deficiency enhances oncogenic features in human colorectal cancer cells via activation of epithelial-mesenchymal transition. *Biomed Res Int*. **2018**:9532389.

Dusoswa SA, Verhoeff J, Abels E, Mendez-Huergo SP, Croci DO, Kuijper LH, de Miguel E, Wouters V, Best MG, Rodriguez E *et al.* 2020. Glioblastomas exploit truncated O-linked glycans for local and distant immune modulation via the macrophage galactose-type lectin. *Proc Natl Acad Sci U S A*. **117**:3693–3703.

Freire T, Osinaga E. 2012. The sweet side of tumor immunotherapy. *Immunotherapy*. **4**:719–734.

Freire T, Bay S, Vichier-Guerre S, Lo-Man R, Leclerc C. 2006. Carbohydrate antigens: Synthesis aspects and immunological applications in cancer. *Mini Rev Med Chem*. **6**:1357–1373.

Freire-de-Lima L, Gelfenbeyn K, Ding Y, Mandel U, Clausen H, Handa K, Hakomori SI. 2011. Involvement of O-glycosylation defining oncofetal fibronectin in epithelial-mesenchymal transition process. *Proc Natl Acad Sci U S A*. **108**:17690–17695.

Freitas D, Campos D, Gomes J, Pinto F, Macedo JA, Matos R, Mereiter S, Pinto MT, Polonia A, Gartner F *et al.* 2019. O-glycans truncation modulates gastric cancer cell signaling and transcription leading to a more aggressive phenotype. *EBioMedicine*. **40**:349–362.

Fu C, Zhao H, Wang Y, Cai H, Xiao Y, Zeng Y, Chen H. 2016. Tumor-associated antigens: Tn antigen, sTn antigen, and T antigen. *HLA*. **88**:275–286.

Garcia-Ortiz A, Serrador JM. 2018. Nitric oxide Signaling in T cell-mediated immunity. *Trends Mol Med*. **24**:412–427.

Garrido-Castro AC, Lin NU, Polyak K. 2019. Insights into molecular classifications of triple-negative breast cancer: Improving patient selection for treatment. *Cancer Discov*. **9**:176–198.

Gill DJ, Tham KM, Chia J, Wang SC, Steentoft C, Clausen H, Bard-Chapeau EA, Bard FA. 2013. Initiation of GalNAc-type O-glycosylation in the endoplasmic reticulum promotes cancer cell invasiveness. *Proc Natl Acad Sci U S A*. **110**:E3152–E3161.

Giuli MV, Giuliani E, Screpanti I, Bellavia D, Checquolo S. 2019. Notch Signaling activation as a Hallmark for triple-negative breast cancer subtype. *J Oncol*. **2019**:8707053.

Glasner A, Plitas G. 2021. Tumor resident regulatory T cells. *Semin Immunol*. **52**:101476.

Gold DV, Mattes MJ. 1988. Monoclonal antibody B72.3 reacts with a core region structure of O-linked carbohydrates. *Tumor Biol*. **9**:137–144.

Gupta N, Gaikwad S, Kaushik I, Wright SE, Markiewski MM, Srivastava SK. 2021. Atovaquone suppresses triple-negative breast tumor growth by reducing immune-suppressive cells. *Int J Mol Sci*. **22**:1–16.

Halasi M, Wang M, Chavan TS, Gaponenko V, Hay N, Gartel AL. 2013. ROS inhibitor N-acetyl-L-cysteine antagonizes the activity of proteasome inhibitors. *Biochem J*. **454**:201–208.

Hofmann BT, Schluter L, Lange P, Mercanoglu B, Ewald F, Folster A, Picksak AS, Harder S, El Gammal AT, Grupp K *et al.* 2015. COSMC knockdown mediated aberrant O-glycosylation promotes oncogenic properties in pancreatic cancer. *Mol Cancer*. **14**:109.

2021. https://www.who.int/cancer/.

Ju T, Lanneau GS, Gautam T, Wang Y, Xia B, Stowell SR, Willard MT, Wang W, Xia JY, Zuna RE *et al.* 2008. Human tumor antigens Tn and sialyl Tn arise from mutations in Cosmc. *Cancer Res*. **68**: 1636–1646.

Julien S, Videira PA, Delannoy P. 2012. Sialyl-tn in cancer: (how) did we miss the target? *Biomol Ther*. **2**:435–466.

Kao J, Ko EC, Eisenstein S, Sikora AG, Fu S, Chen SH. 2011. Targeting immune suppressing myeloid-derived suppressor cells in oncology. *Crit Rev Oncol Hematol*. **77**:12–19.

Kawaguchi T, Takazawa H, Imai S, Morimoto J, Watanabe T, Kanno M, Igarashi S. 2006. Expression of Vicia villosa agglutinin (VVA)-binding glycoprotein in primary breast cancer cells in relation to lymphatic metastasis: is atypical MUC1 bearing Tn antigen a receptor of VVA? *Breast Cancer Res Treat*. **98**: 31–43.

Kjeldsen T, Clausen H, Hirohashi S, Ogawa T, Iijima H, Hakomori S. 1988. Preparation and characterization of monoclonal antibodies directed to the tumor-associated O-linked sialosyl-2-–6 alpha-N-acetylgalactosaminyl (sialosyl-Tn) epitope. *Cancer Res*. **48**: 2214–2220.

Kolbl AC, Jeschke U, Friese K, Andergassen U. 2016. The role of TF- and Tn-antigens in breast cancer metastasis. *Histol Histopathol*. **31**: 613–621.

Konska G, Guerry M, Caldefie-Chezet F, De Latour M, Guillot J. 2006. Study of the expression of Tn antigen in different types of human breast cancer cells using VVA-B4 lectin. *Oncol Rep*. **15**:305–310.

Kramer MG, Masner M, Casales E, Moreno M, Smerdou C, Chabalgoity JA. 2015. Neoadjuvant administration of Semliki Forest virus expressing interleukin-12 combined with attenuated salmonella eradicates breast cancer metastasis and achieves long-term survival in immunocompetent mice. *BMC Cancer*. **15**:620.

Kudelka MR, Ju T, Heimburg-Molinaro J, Cummings RD. 2015. Simple sugars to complex disease–mucin-type O-glycans in cancer. *Adv Cancer Res*. **126**:53–135.

Li D, Romain G, Flamar AL, Duluc D, Dullaers M, Li XH, Zurawski S, Bosquet N, Palucka AK, Le Grand R *et al.* 2012. Targeting self- and foreign antigens to dendritic cells via DC-ASGPR generates IL-10-producing suppressive CD4+ T cells. *J Exp Med*. **209**:109–121.

Liu Z, Liu J, Dong X, Hu X, Jiang Y, Li L, Du T, Yang L, Wen T, An G *et al.* 2019. Tn antigen promotes human colorectal cancer metastasis via H-Ras mediated epithelial-mesenchymal transition activation. *J Cell Mol Med*. **23**:2083–2092.

Maj T, Wang W, Crespo J, Zhang H, Wang W, Wei S, Zhao L, Vatan L, Shao I, Szeliga W *et al.* 2017. Oxidative stress controls regulatory T cell apoptosis and suppressor activity and PD-L1-blockade resistance in tumor. *Nat Immunol*. **18**:1332–1341.

Matsumoto Y, Zhang Q, Akita K, Nakada H, Hamamura K, Tsuchida A, Okajima T, Furukawa K, Urano T, Furukawa K. 2013. Trimeric Tn antigen on syndecan 1 produced by ppGalNAc-T13 enhances cancer metastasis via a complex formation with integrin alpha5beta1 and matrix metalloproteinase 9. *J Biol Chem*. **288**: 24264–24276.

Mereiter S, Balmana M, Campos D, Gomes J, Reis CA. 2019. Glycosylation in the era of cancer-targeted therapy: Where are we heading? *Cancer Cell*. **36**:6–16.

Minai-Tehrani A, Chang SH, Park SB, Cho MH. 2013. The Oglycosylation mutant osteopontin alters lung cancer cell growth and migration in vitro and in vivo. *Int J Mol Med*. **32**:1137–1149.

Munkley J, Elliott DJ. 2016. Hallmarks of glycosylation in cancer. *Oncotarget*. **7**:35478–35489.

Nguyen AT, Chia J, Ros M, Hui KM, Saltel F, Bard F. 2017. Organelle specific O-glycosylation drives MMP14 activation, tumor growth, and metastasis. *Cancer Cell*. **32**:639:e636–e653.

Osinaga E, Bay S, Tello D, Babino A, Pritsch O, Assemat K, Cantacuzene D, Nakada H, Alzari P. 2000. Analysis of the fine specificity of Tn-binding proteins using synthetic glycopeptide epitopes and a biosensor based on surface plasmon resonance spectroscopy. *FEBS Lett*. **469**:24–28.

Park JH, Nishidate T, Kijima K, Ohashi T, Takegawa K, Fujikane T, Hirata K, Nakamura Y, Katagiri T. 2010. Critical roles of mucin 1 glycosylation by transactivated polypeptide N-acetylgalactosaminyltransferase 6 in mammary carcinogenesis. *Cancer Res*. **70**:2759–2769.

Park SY, Choi JH, Nam JS. 2019. *Targeting Cancer Stem Cells in Triple-Negative Breast Cancer*. Cancers (Basel). **11**,**965**:1–30; doi: 10.3390/cancers11070965.

Peixoto A, Relvas-Santos M, Azevedo R, Santos LL, Ferreira JA. 2019. Protein glycosylation and tumor microenvironment alterations driving cancer hallmarks. *Front Oncol*. **9**:380.

Persson N, Stuhr-Hansen N, Risinger C, Mereiter S, Polonia A, Polom K, Kovacs A, Roviello F, Reis CA, Welinder C *et al.* 2017. Epitope mapping of a new anti-Tn antibody detecting gastric cancer cells. *Glycobiology*. **27**:635–645.

Pinho SS, Reis CA. 2015. Glycosylation in cancer: Mechanisms and clinical implications. *Nat Rev Cancer*. **15**:540–555.

Prendergast JM, Galvao da Silva AP, Eavarone DA, Ghaderi D, Zhang M, Brady D, Wicks J, DeSander J, Behrens J, Rueda BR. 2017. Novel anti-Sialyl-Tn monoclonal antibodies and antibody-drug conjugates demonstrate tumor specificity and anti-tumor activity. *MAbs*. **9**: 615–627.

Pulaski BA, Ostrand-Rosenberg S. 1998. Reduction of established spontaneous mammary carcinoma metastases following immunotherapy with major histocompatibility complex class II and B7.1 cell-based tumor vaccines. *Cancer Res*. **58**:1486–1493.

Pulaski BA, Ostrand-Rosenberg S. 2001. Mouse 4T1 breast tumor model. *Curr Protoc Immunol*Chapter 20.

Pulaski BA, Terman DS, Khan S, Muller E, Ostrand-Rosenberg S. 2000. Cooperativity of staphylococcal aureus enterotoxin B superantigen, major histocompatibility complex class II, and CD80 for immunotherapy of advanced spontaneous metastases in a clinically relevant postoperative mouse breast cancer model. *Cancer Res*. **60**: 2710–2715.

Radhakrishnan P, Dabelsteen S, Madsen FB, Francavilla C, Kopp KL, Steentoft C, Vakhrushev SY, Olsen JV, Hansen L, Bennett EP *et al.* 2014. Immature truncated O-glycophenotype of cancer directly induces oncogenic features. *Proc Natl Acad Sci U S A*. **111**: E4066–E4075.

Reddish MA, Jackson L, Koganty RR, Qiu D, Hong W, Longenecker BM. 1997. Specificities of anti-sialyl-Tn and anti-Tn monoclonal antibodies generated using novel clustered synthetic glycopeptide epitopes. *Glycoconj J*. **14**:549–560.

Redig AJ, McAllister SS. 2013. Breast cancer as a systemic disease: A view of metastasis. *J Intern Med*. **274**:113–126.

Saeland E, van Vliet SJ, Backstrom M, van den Berg VC, Geijtenbeek TB, Meijer GA, van Kooyk Y. 2007. The C-type lectin MGL expressed by dendritic cells detects glycan changes on MUC1 in colon carcinoma. *Cancer Immunol Immunother*. **56**:1225–1236.

Scimeca M, Urbano N, Bonfiglio R, Duggento A, Toschi N, Schillaci O, Bonanno E. 2019. Novel insights into breast cancer progression and metastasis: A multidisciplinary opportunity to transition from biology to clinical oncology. *Biochim Biophys Acta Rev Cancer*. **1872**:138–148.

Steentoft C, Vakhrushev SY, Joshi HJ, Kong Y, Vester-Christensen MB, Schjoldager KT, Lavrsen K, Dabelsteen S, Pedersen NB, Marcos-Silva L *et al.* 2013. Precision mapping of the human O-GalNAc glycoproteome through simple cell technology. *EMBO J*. **32**:1478–1488.

Thomas M, Kelly ED, Abraham J, Kruse M. 2019. Invasive lobular breast cancer: A review of pathogenesis, diagnosis, management, and future directions of early stage disease. *Semin Oncol*. **46**: 121–132.

van Vliet SJ, Gringhuis SI, Geijtenbeek TB, van Kooyk Y. 2006. Regulation of effector T cells by antigen-presenting cells via interaction of the C-type lectin MGL with CD45. *Nat Immunol*. **7**: 1200–1208.

Yin L, Duan JJ, Bian XW, Yu SC. 2020. Triple-negative breast cancer molecular subtyping and treatment progress. *Breast Cancer Res*. **22**:61.

Yoo NJ, Kim MS, Lee SH. 2008. Absence of COSMC gene mutations in breast and colorectal carcinomas. *APMIS*. **116**:154–155.

Zhang LJ, Huang R, Shen YW, Liu J, Wu Y, Jin JM, Zhang H, Sun Y, Chen HZ, Luan X. 2021. Enhanced anti-tumor efficacy by inhibiting HIF-1alpha to reprogram TAMs via core-satellite upconverting nanoparticles with curcumin mediated photodynamic therapy. *Biomater Sci*. **9**:6403–6415.